

Thomas Prisner · Sevdalina Lyubenova · Yener Atabay
Fraser MacMillan · Achim Kröger · Oliver Klimmek

Multifrequency cw-EPR investigation of the catalytic molybdenum cofactor of polysulfide reductase from *Wolinella succinogenes*

Received: 5 September 2002 / Accepted: 11 November 2002 / Published online: 17 January 2003
© SBIC 2003

Abstract Electron paramagnetic resonance (EPR) spectra of the molybdenum centre in polysulfide reductase (Psr) from *Wolinella succinogenes* with unusually high G -tensor values have been observed for the first time. Three different Mo^{V} states have been generated (by the addition of the substrate polysulfide and different redox agents) and analysed by their G - and hyperfine tensors using multifrequency (S-, X- and Q-band) cw-EPR spectroscopy. The unusually high G -tensor values are attributed to a large number of sulfur ligands. Four sulfur ligands are assumed to arise from two pterin cofactors; one additional sulfur ligand was identified from mutagenesis studies to be a cysteine residue of the protein backbone. One further sulfur ligand is proposed for two of the Mo^{V} states, based on the experimentally observed shift of the g_{av} value. This sixth sulfur ligand is postulated to belong to the polysulfide substrate consumed within the catalytic reaction cycle of the enzyme. The influence of the co-protein sulfur transferase on the Mo^{V} G -tensor supports this assignment.

Keywords Molybdoenzymes · Molybdopterin · G -tensor · Q-band EPR · S-band EPR

Introduction

ATP formation from ADP and inorganic phosphate is coupled to electron transport in many anaerobic

prokaryotes [1, 2, 3, 4]. Electron transport is catalysed by electron transport chains within the membrane of these organisms, and is coupled to the generation of an electrochemical proton potential across the membrane that drives ATP synthesis. These processes are termed anaerobic respiration, since O_2 is replaced by other terminal electron acceptors such as nitrate, fumarate or polysulfide. Anaerobic respiration with polysulfide is termed polysulfide respiration and has been most thoroughly studied in *Wolinella succinogenes* [2, 5, 6]. *W. succinogenes* grows via polysulfide respiration with H_2 or formate as electron donors. The electron transport chain catalysing these reactions consists of polysulfide reductase (Psr) and either hydrogenase or formate dehydrogenase, which are integrated into the bacterial membrane.

Isolated Psr catalyses the reduction of polysulfide to sulfide with borohydride, and the oxidation of sulfide to polysulfide with 2,3-dimethyl-1,4-naphthoquinone [2, 6]. The enzyme is made up of three different subunits, PsrA, PsrB and PsrC. The catalytic subunit PsrA carries a molybdenum ion bound to two molybdopterin guanine dinucleotides (MGD), where the reduction of polysulfide or the oxidation of sulfide takes place, and an FeS centre. PsrB mediates electron transfer from the membrane anchor PsrC to PsrA via its four FeS centres.

According to its amino acid sequence, the catalytic subunit PsrA belongs to the DMSO reductase family of molybdo-oxidoreductases [7, 8]. The crystal structures of several single polypeptide enzymes of this family have been determined [8]. In all these enzymes the Mo ion is coordinated by two MGD molecules and appears to serve as the direct electron donor to or acceptor from the respective substrates. In DMSO reductase a serine residue of the protein is identified as a further ligand to the Mo ion [9, 10], whereas this ligand is identified to be a cysteine in nitrate reductase [11] and in formate dehydrogenase [12].

Additionally, Mo K-edge extended X-ray absorption fine structure spectroscopy (EXAFS) and EPR spectroscopy have been applied to these molybdenum

T. Prisner (✉) · S. Lyubenova · Y. Atabay · F. MacMillan
Institute of Physical and Theoretical Chemistry,
Johann Wolfgang Goethe-University Frankfurt,
Marie-Curie-Strasse 11, 60439 Frankfurt am Main, Germany
E-mail: prisner@chemie.uni-frankfurt.de
Fax: +49-69-79829404

A. Kröger · O. Klimmek
Institute of Microbiology,
Johann Wolfgang Goethe-University Frankfurt,
Marie-Curie-Strasse 9,
60439 Frankfurt am Main, Germany

enzymes to further characterise the Mo centre in the different oxidation states (Mo^{IV} , Mo^{V} and Mo^{VI}) within the catalytic cycle.

EXAFS spectroscopy has been used to probe the environment of the Mo ion in DMSO reductase from *Rhodobacter capsulatus* and *Rhodobacter sphaeroides* [13, 14] and of nitrate reductase from *Paracoccus denitrificans* [15] in its diamagnetic Mo^{IV} and Mo^{VI} oxidation states. In agreement with the crystallographic results, the EXAFS data show that four S atoms (considered to arise from the dithiolene groups of the two MGD) and either an O atom from a serine residue or an S atom from a cysteine residue are ligated to the Mo ion in these enzymes.

EPR spectroscopy is a well-established method for studying paramagnetic centres in enzymes. The paramagnetic Mo^{V} state ($S=1/2$) is easily observed by EPR and has been widely used to investigate the coordination of molybdenum centres in proteins [16, 17, 18].

Molybdenum occurs naturally in a variety of isotopes, of which ^{95}Mo and ^{97}Mo have a nuclear spin ($I=5/2$) with a combined natural abundance of $\sim 25.5\%$ (^{95}Mo , 15.9%; ^{97}Mo , 9.6%). This fact can be used to unequivocally assign EPR spectra, as these isotopes will result in a strong anisotropic Mo hyperfine coupling characteristic for molybdenum [19].

It has been shown that in inorganic Mo^{V} complexes the average G -tensor value g_{av} is sensitive to the covalency of the metal-ligand bond and therefore to the nature of the ligands [20]. In addition, spin-orbit coupling influences the G -tensor anisotropy (ΔG), depending on the symmetry of the metal coordination sphere [21]. Thus, detailed analysis of EPR spectra can provide valuable information on the ligand sphere of the Mo^{V} state. The ligand symmetry and the covalency of the ligand bonds also influence the hyperfine tensor of the ^{95}Mo and ^{97}Mo isotopes.

Ligands in the first and second coordination spheres of the metal ion can often be directly identified via their hyperfine coupling. This has been demonstrated for ^{17}O [22, 23, 24], ^{31}P [25], ^{13}C [26] and ^{33}S [20, 27] in the first coordination sphere and for ^1H and ^2H in the second coordination sphere [20, 28]. The anisotropic and isotropic parts of these hyperfine tensors give valuable information on the structural arrangement of these ligands in the complex [20]. For small hyperfine couplings of nuclei in the second coordination sphere, normally not resolved in the cw-EPR spectra of disordered frozen solution samples, pulsed EPR (ESEEM: electron spin echo envelope modulation) [29] and ENDOR (electron nuclear double resonance) [26, 28, 30] experiments are required.

In order to distinguish between hyperfine and G -tensor interactions, multifrequency EPR can also be applied. This approach has been used on xanthine oxidase and other molybdenum-containing hydroxylases to distinguish differences in the coordination spheres of the metal in its Mo^{V} states [31].

In this work we used multifrequency cw-EPR to characterise the Mo^{V} states in Psr from *W. succinogenes*.

It has been postulated that the Mo ion in the catalytic centre of Psr alternates between the oxidation states IV, V and VI during turnover. Three Mo^{V} species with different spectroscopic properties have been detected and their EPR parameters have been analysed by numerical simulation. The similarity of these parameters with other enzymes of the DMSO reductase family (with known X-ray structures) allows the assignment of the Mo^{V} ligand sphere in Psr. Additionally, the observed shift of the g_{av} value between different Mo^{V} states and the alteration of ΔG for one of these states after binding of sulfur transferase (Sud) to Psr leads to the assumption that this state is the polysulfide substrate-bound Mo^{V} transition state of the catalytic reaction.

Materials and methods

Growth of *Wollinella succinogenes*

W. succinogenes was grown in a medium containing fumaric acid (90 mM), sodium formate (100 mM), K_2HPO_4 (20 mM), $(\text{NH}_4)_2\text{SO}_4$ (5 mM), sodium acetate (20 mM), glutamate (1 mM), and Tris-KOH (50 mM, pH 7.8). After the addition of MgCl_2 (0.25 mM), CaCl_2 (0.05 mM), and a trace element solution (2 mL L^{-1}), the medium was sterilised, flushed with N_2 , inoculated (0.4%) and kept at 37 °C until the cell density was about 10^{12} L^{-1} (about 17 h).

The trace element solution contained (mg L^{-1}) disodium EDTA (5200), $\text{FeCl}_2 \cdot 4\text{H}_2\text{O}$ (1500), ZnCl_2 (70), $\text{MnCl}_2 \cdot 4\text{H}_2\text{O}$ (100), H_3BO_3 (62), $\text{CoCl}_2 \cdot 6\text{H}_2\text{O}$ (190), $\text{CuCl}_2 \cdot 2\text{H}_2\text{O}$ (17), $\text{NiCl}_2 \cdot 6\text{H}_2\text{O}$ (24) and $\text{Na}_2\text{MoO}_4 \cdot 2\text{H}_2\text{O}$ (36).

Purification of the PsrABC complex

All the following steps were performed with anoxic buffers at 0 °C. Cells of *W. succinogenes* grown with formate and fumarate were harvested in the exponential growth phase and were suspended (40 g cell protein L^{-1}) in a buffer containing 50 mM potassium phosphate and 1 mM dithiothreitol (pH 7.3) at 0 °C (buffer A). The suspension was passed through a French press at 130 Mpa with a flow rate of 10 mL min^{-1} . The resulting cell homogenate was centrifuged for 35 min at 100,000 $\times g$ to yield the soluble cell fraction (supernatant) and the membrane fraction. The membrane fraction was suspended in buffer A (20 g membrane protein L^{-1}) containing, in addition, 0.6 g Triton X-100 and 0.2 g n-dodecyl- β -D-maltoside g^{-1} membrane protein. The suspension was stirred for 90 min at 0 °C. After centrifugation (40 min at 100,000 $\times g$) the supernatant was applied to an anion-exchange column (DEAE-Sepharose CL-6B; Pharmacia Biotech) equilibrated with buffer A containing, in addition, 0.05% (v/v) Triton X-100. Under these equilibrium conditions the enzyme activity was eluted by washing the column with equilibrium buffer, whereas about two-thirds of the extracted membrane protein remained on the column. The fractions containing the enzyme activity were combined and then concentrated by pressure dialysis using a 50-kDa filter (Amicon) in a dialysis chamber. By repeated dilution and concentration (three times) of the protein, the buffer was replaced by a buffer containing 50 mM Tris chloride and 1 mM dithiothreitol (pH 8.1) at 0 °C (buffer B). The concentrated protein was then applied for a second time to an anion-exchange column (DEAE-Sepharose CL-6B; Pharmacia Biotech) equilibrated with buffer B containing, in addition, 0.05% (v/v) Triton X-100. After a washing with this equilibration buffer, elution was performed by a linear sodium chloride gradient (0–200 mM). The fractions containing the enzyme activity were combined and then concentrated by pressure

dialysis using a 50-kDa filter and were desalted by repeated dilution and concentration (three times) of the protein with buffer B. The concentrated Psr complex was frozen and stored in liquid N₂.

Preparation of EPR samples

Samples were prepared under anaerobic conditions (argon) by freezing of ca. 100 μ L of sample in quartz EPR tubes (o.d. 4 mm, Wilmad). Psr concentration was usually 130–150 μ M. The following redox agents were used to either oxidize or reduce the protein: Na₂S (200 μ M–6 mM), Na₂S₄O₄ (2 mM), NaBH₄ (20 mM), polysulfide (S_n) (50 μ M–2 mM) in sulfide-containing solutions.

EPR spectroscopy

X-Band cw-EPR spectra were recorded on a Bruker ESP300E spectrometer using a standard rectangular Bruker EPR cavity (ER4102T) equipped with an Oxford helium cryostat (ESR900). The microwave frequency was measured using a Systron Donner frequency counter (6054D), and the magnetic field was measured using a Bruker gaussmeter (ER035M). The Q-band EPR measurements were performed on a Bruker ELEXSYS E500 spectrometer equipped with a Bruker Q-band microwave bridge, a Bruker Q-band EPR resonator (ER5103QTH) and an Oxford cryostat (CF935). S-band cw-EPR spectra were recorded on a home-built pulsed and cw S-band spectrometer using a Bruker (ER 4118S-MS-5W1) probehead and an Oxford cryostat (CF935).

All EPR-spectra were recorded at 120 K. Absolute signal intensities were determined by comparing double integrated spectra with various known standards (Cu-EDTA, CuSO₄, Tempo). The magnetic field was calibrated using a DPPH standard sample.

cw-EPR spectra simulation

Quantitative interpretation of the cw-EPR spectra were performed with a home-written simulation and fit program, written in Matlab. This program takes into account the naturally abundant isotopes of Mo (Mo \sim 74.5%, with nuclear spin $I=0$; ⁹⁵Mo and ⁹⁷Mo \sim 25.5%, with nuclear spin $I=5/2$) with their different hyperfine contributions to the spectrum. Additionally, it allows the simultaneous simulation of two different Mo^V species (1 and 2) with relative intensities α and β . This is necessary because, under some of the chosen redox conditions of the protein, admixtures of two Mo^V species are observed (see Results and Discussion). In this case, for each molybdenum species the G -tensor and the molybdenum hyperfine tensor A_{Mo} can be chosen independently. An additional hyperfine coupling tensor A to a proton nuclear spin may also be included for the simulation of spectra with additional observable splittings (see Results and Discussion).

The corresponding spin Hamiltonian H for two molybdenum species is given by:

$$H = \alpha \cdot H(1) + \beta \cdot H(2) \quad (1)$$

whereby $H(1)$ is the spin Hamiltonian for species 1:

$$H(1) = \vec{B}_0 \cdot \vec{G}_1 \cdot \vec{S}_1 + \vec{S}_1 \cdot \vec{A}_{\text{Mol}} \cdot \vec{I}_{\text{Mol}} + \vec{S}_1 \cdot \vec{A}_1 \cdot \vec{I}_1 \quad (2)$$

Here the first term describes the Zeeman interaction of the unpaired electron spin ($S=1/2$) with the external magnetic field, the second term the Mo hyperfine interaction for the naturally abundant Mo isotopes (nuclear spin $I=5/2$) and the third term includes an additional hyperfine interaction with a ligand nucleus. $H(2)$ has the same terms for the second species 2.

The computation of magnetic field resonance conditions is based on a high-field approximation solution for the Mo^V spin system: G - and hyperfine-tensor contributions to the resonance frequency are calculated by second-order perturbation theory for a fixed magnetic field (centre of the spectra) and converted to a

field-swept spectra representation. The powder average for the disordered frozen solution spectra is calculated by summation over approximately 1000 orientations (uniformly distributed orientations on a half sphere) of the external magnetic field with respect to the molecular axis system. The resulting powder spectra for each species is then convoluted with an inhomogeneous Gaussian line-shape (with \sim 5 G peak-to-peak linewidth for the simulations shown below). Obviously, quadrupole tensor spectral contributions from forbidden EPR transitions of the ⁹⁷Mo isotope (\sim 10% natural abundance) are not included at this level of approximation. Additionally, the ⁹⁵Mo and ⁹⁷Mo hyperfine tensors are taken as collinear with the G -tensor axis system.

In a second step, after an approximate set of parameters is found for the spectra by simulation, a Simplex fit routine with simulated annealing is used to obtain the minimum least-square solutions for the parameters and an estimate of the error.

Results

Figure 1A shows the experimental X-band cw-EPR spectrum obtained for a frozen solution of Psr treated with sodium dithionite, together with a simulation (Fig. 1B) using the theoretical model described above. Despite the fact that the spectra are centred at a very low magnetic field (respectively having an unusually high g_{av} value), the signal can be assigned quantitatively and unequivocally to a Mo^V species due to the specific hyperfine peaks arising from the ⁹⁵Mo and ⁹⁷Mo isotopes with a nuclear spin $I=5/2$. These lines are best resolved at the low-field edge of the EPR spectra and are enlarged in the insert in Fig. 1. The simulation of the overall EPR

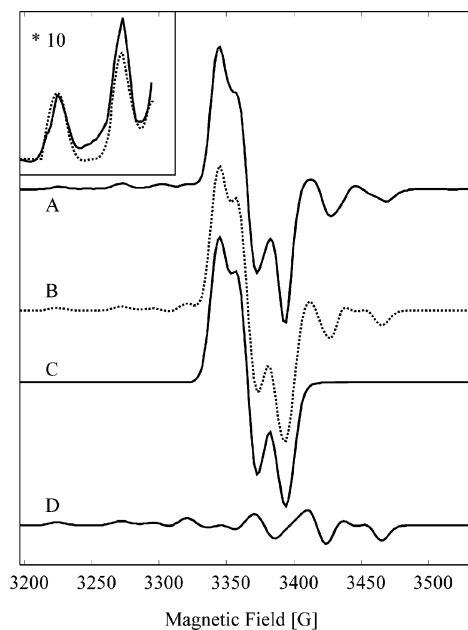


Fig. 1 Mo^V X-band cw-EPR signal of Psr, after reaction with sodium dithionite (Very-High- G state) measured at 120 K. The experimental spectrum (A) is shown as a solid line and the simulation of this spectrum (B) as a dotted line. For a better understanding of the spectra, the simulations for the different Mo isotopes [with (C) and without (D) Mo hyperfine coupling] are shown separately below. The insert shows the two outermost Mo hyperfine lines on an enlarged scale

signal reproduces the natural isotope abundance ratios of Mo (Mo, 74.5%, $I=0$; $^{95}\text{Mo}/^{97}\text{Mo} \sim 25.5\%$, $I=5/2$). The contributions to the overall spectra from Mo isotopes without and with nuclear spin are disentangled in Fig. 1C and Fig. 1D for illustration. The Mo hyperfine coupling could be satisfactorily simulated with a hyperfine tensor $A_{\text{Mo}} = (20, 20, 50)$ G.

Three spectroscopically different Mo^{V} species were observed, depending on preparative conditions. They are depicted together with the respective simulations in Fig. 2. These states, called Very-High- G , Very-High- G /split and High- G , can be distinguished by their G -tensor values which are summarized in Table 1 and are described in the following.

Very-High- G

This signal was observed for preparations of Psr with an excess of the substrate polysulfide (Fig. 2A and Table 1), but could also be generated by incubation of Psr samples with the reducing agent sodium dithionite ($\text{Na}_2\text{S}_2\text{O}_4$) (see Fig. 1). The g_{av} value of these spectra is among the highest observed for Mo enzymes.

For preparations with the coenzyme Sud present, the same signal is observed for high concentrations of the substrate polysulfide (2 mM), whereas for lower concentrations of polysulfide (300 μM) a slight change in ΔG was observed. The spectra and G -tensor values of this preparation, labelled Very-High- G /Sud, are shown in Fig. 2B and Table 1. Although this slight change of ΔG was already obtained by fitting of the X-band spectra, it could be much better resolved by Q-band EPR measurements as shown in Fig. 3. In this case the change of ΔG could directly be determined from the spectra. The same parameters were obtained for the X-band and Q-band simulations.

Very-High- G /split

This Mo^{V} species with a strongly altered G -tensor anisotropy (ΔG) and rhombicity ε , defined as:

$$\varepsilon = \frac{g_{zz} - g_{yy}}{\Delta G} \quad (3)$$

was observed for the Psr enzyme incubated with sodium borohydride (NaBH_4) (Fig. 2C and Table 1). The g_{av} value is unaltered for this species with respect to the Very-High- G state, but the rhombicity ε of the G -tensor has changed to an axial G -tensor. An additional splitting

is observed on the low-field (g_{zz}) peak of the spectra. This splitting arises from an additional hyperfine interaction to the Mo^{V} ion, as can be shown by the field independence of this splitting. Multifrequency EPR measurements performed at S- (3 GHz), X- (9 GHz) and Q-band (34 GHz) frequencies for this preparation are shown in Fig. 4. The spectra can be simulated with the G -tensor given in Table 1 and an additional hyperfine splitting of $A = (2, 2, 8)$ G.

High- G

Finally, a further Mo^{V} species was identified, most clearly observable for samples incubated only with Na_2S . For this signal the g_{av} is lower with respect to the Very-High- G species described above by $\delta g_{\text{av}} \approx 0.015$. Nevertheless, even this g_{av} value is still rather high compared to most Mo^{V} species reported in the literature. Contributions from this species were observable for

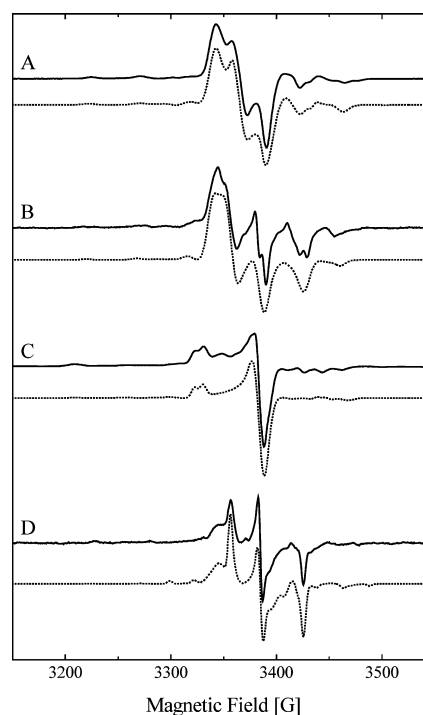


Fig. 2 X-band cw-EPR signals of different Mo^{V} species: (A) Very-High- G ; (B) Very-High- G /Sud; (C) Very-High- G /split; (D) High- G . *Solid lines*: experimental spectra (measured at 120 K). *Dotted lines*: simulations of the experimental spectra with the simulation parameters given in Table 1

Table 1 G -Tensor values of the observed Mo^{V} species in Psr. Error is ± 0.001 for all G -tensor absolute values

State (preparation)	g_{av}	$\Delta G \times 10^{-3}$	g_{xx}	g_{yy}	g_{zz}	Rhombicity $\varepsilon = (g_{zz} - g_{yy})/\Delta G$
Very-High- G (polysulfide)	2.0021	291	1.9874	2.0025	2.0165	0.47
Very-High- G /Sud (polysulfide + Sud)	2.0024	280	1.9872	2.0049	2.0152	0.36
Very-High- G /split (borohydride)	2.0023	355	1.9905	1.9905	2.0260	1.00
High- G (Na_2S)	1.9889	405	1.9675	1.9911	2.0080	0.43

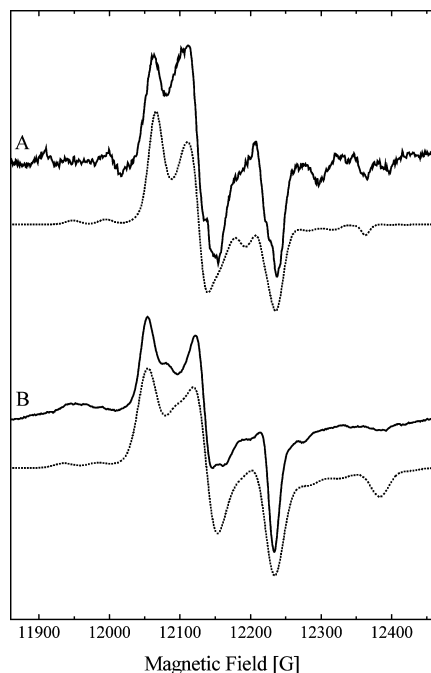


Fig. 3 Q-band EPR spectra of Psr after treatment with polysulfide: (A) with Sud (Very-High-G/Sud); (B) without Sud (Very-High-G). The experimental spectra are shown as *solid lines* and the simulations with parameters described in Table 1 are shown as *dotted lines* below

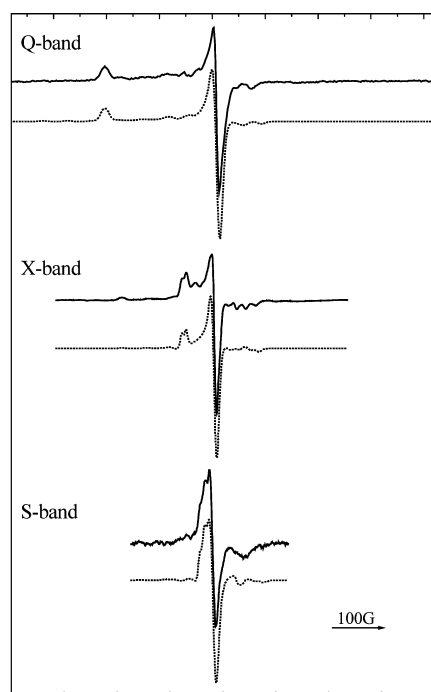


Fig. 4 Multifrequency cw-EPR spectra (Q-, X-, S-band) of Psr incubated with borohydride (Very-High-G/split). The simulations at all frequencies are performed with an additional hyperfine splitting of 8 G. For the simulation of the Q-band spectrum a slightly larger line width (7 versus 4 G) was used

many of the described preparations, most visible at the high-field edge of the experimental spectra (see Fig. 2D). It was observed that this signal increased for samples after numerous short partial freeze-thaw cycles. The relative contribution of this signal for the different preparations is given in Table 2.

The absolute concentration of the Mo^V states was determined by double integration of the total Mo^V EPR signal and comparing these values with calibrated standard samples (see Material and methods), measured under similar conditions. These concentrations are tabulated relative to the enzyme concentration in Table 2.

Discussion

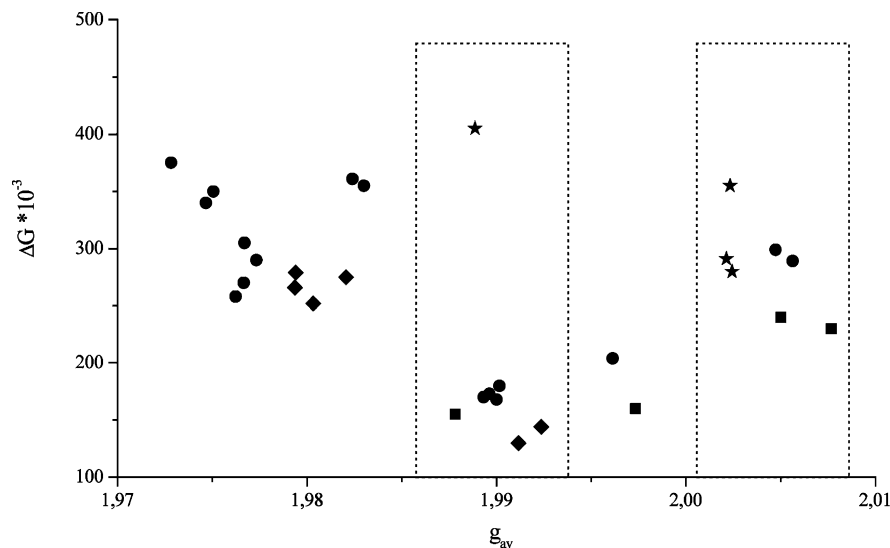
The observed Very-High-G Mo^V species have g_{av} values unusually high as compared with previously observed molybdenum enzymes, similar only to Very-High-G states of periplasmatic and assimilatory nitrate reductases [15, 32] and formate dehydrogenase [33, 34, 35]. For all these enzymes it is known, from X-ray crystallography of the Mo^{IV} state of the enzyme, that the Mo centre is coordinated to four equatorial dithiolene sulfur atoms from a pair of MGDs and to another sulfur atom from a cysteine residue. Accordingly, the unusually high g_{av} value of the Mo^V states of these enzymes is attributed to the large number of sulfur ligands. An increase of the g_{av} value by exchanging an oxygen to a sulfur ligand of Mo^V ions has been experimentally and theoretically thoroughly investigated [14, 21, 36] and is mainly due to the covalency of the metal-ligand bonds. Both the g_{av} and the ΔG values are very similar for these states, as can be seen in Fig. 5. The ratio of these two values is correlated to the coordination symmetry of the metal complex; therefore the nature and structure of the ligands in Psr should be very similar to nitrate reductase and formate dehydrogenase.

The difference of the g_{av} values between the Very-High-G species and the High-G species observed in Psr matches exactly the value δg_{av} expected for an exchange of an oxygen to a sulfur ligand found as described above [21]. The same change in g_{av} has been observed in DMSO reductase for a site-directed mutation Ser147 → Cys [14]. Consistent with the expected five sulfur ligands, the g_{av} value of this mutant is very close to the g_{av} value of the

Table 2 Mo^V concentration with respect to Psr enzyme concentration (130–150 μ M) and relative content of the High-G state for the different preparations

Preparation	% Mo ^V total	% High-G
Polysulfide	20	2
Polysulfide + Sud	10	1
Dithionite	20	<1
Borohydride	20	<1
Na ₂ S	10	7
Polysulfide + Na ₂ S	20	10
Without redox agents	~2	~1

Fig. 5 Correlation of the G -tensor anisotropy ΔG with the average G -tensor value g_{av} for some observed Mo^V states of the DMSO reductase family. Stars: polysulfide reductase; circles: nitrate reductase; squares: formate dehydrogenase; diamonds: DMSO reductase. The two dotted boxes enclose the High- G states (left box) and Very-High- G (right box). The three Very-High- G states of Psr are (ordered by increasing ΔG): Very-High- G /Sud, Very-High- G , Very-High- G /split. The DMSO state in the High- G box belongs to the mutant S147C; the two states between the two boxes belong to cyanide-inhibited enzymes



High- G species observed in nitrate reductase, formate dehydrogenase and Psr. In all these enzymes it is possible to switch between the two states, Very-High- G and High- G , by addition of redox agents or substrate. In Psr the High- G signal could be quantitatively converted to the Very-High- G signal by addition of sodium dithionite.

The nature of the sixth ligand to the Mo^V in Very-High- G states is less clear from EPR spectroscopy. X-ray structures of the Mo^{IV} or Mo^{VI} states of nitrate reductase, formate dehydrogenase and DMSO reductase show one oxo ligand for these states. For all these enzymes, direct ligation of the substrate to the Mo ion via an oxygen atom is discussed for the Mo^V transition state. The possibility of having an oxygen ligand of the High- G state exchanged to a sulfur ligand in the Very-High- G state to explain the shift in g_{av} is discussed for nitrate reductases and formate dehydrogenase, but not favoured because of the better agreement of five sulfur ligands with EXAFS measurements [15]. Structural changes of the Mo^V ligand sphere, which can change not only ΔG but also the g_{av} value [21], are postulated to account for the observed change in g_{av} .

Interestingly, the G -tensor asymmetry ΔG of the Very-High- G state in Psr is slightly altered by the addition of the coprotein Sud (for low concentrations of polysulfide). The function of this coprotein is known from other studies to decrease the Michaelis constant of the Psr at concentrations of polysulfide substrate lower than $100 \mu\text{M}$ [37]. MALDI mass spectrometry has shown that the polysulfide substrate binds specifically to a cysteine residue (Cys109) of the Sud protein [38] and NMR spectroscopy has been used to solve the structure of the Sud dimer and to study its specific interaction surface with Psr upon binding (Rüterjans H, unpublished results). In this bound complex state the transfer of sulfur from polysulfide to the active site of Psr is postulated to occur. The lowering of the Michaelis constant may be due to different aspects of the interaction of Sud on the catalytic cycle (or some combination

of them): (1) Sud could more efficiently collect polysulfide and guide the substrate to the active site of Psr; (2) Sud could increase the contact time between substrate and active centre and therefore the probability of the forward reaction taking place; and (3) Sud could lower the activation energy for the transition state via its interaction with the protein.

The altering of ΔG and of the rhombicity ϵ for the Very-High- G state due to the Sud coprotein could be caused by a slight change in the geometry of the Mo^V ligand sphere. This would imply a binding of the Sud protein to Psr close to the Mo centre for the Very-High- G /Sud state. If the change in the electronic properties of the Mo centre caused by the Sud protein also effects the polysulfide affinity as described above, or is only a result of a steric interaction between Psr and Sud without influence on the catalytic rate constants, has still to be investigated by stopped-flow experiments under turnover conditions. In any case, we believe that the effect of the Sud coprotein on the Very-High- G state indicates that this state is involved in the native catalytic reaction cycle of Psr. In this case, sulfur from the transferred polysulfide could become the sixth ligand to the Mo ion and explain directly the very high g_{av} value of the Very High- G state and the shift δg_{av} with respect to the High- G state.

In contrast to the Very High- G state in Psr, an additional hyperfine coupling of approximately 6 G is observed for the Very-High- G states in nitrate reductases and formate dehydrogenase [15, 33]. This coupling is attributed to indirect coupling to a proton; therefore an OH is assumed in both cases as the sixth ligand. No such additional hyperfine coupling is observed in Psr for the Very-High- G and Very High- G /Sud spectra, again in agreement with the hypothesis that polysulfide serves as the sixth ligand to this Mo^V state in Psr.

Such an additional hyperfine splitting is only observed on the g_{zz} edge of the Very-High- G /split state of Psr. The experimental conditions to create this state

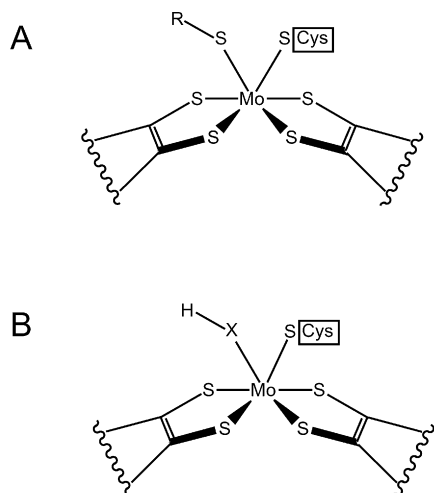


Fig. 6 Proposed structures for the observed Mo^{V} states in Psr: (A) Very-High- G ; (B) Very-High- G /split ($X = \text{S}$ or O)

are less clear; only after long incubation at room temperature with excess of borohydride (and possible contact with oxygen) could spectra with an almost axial symmetry be observed. The resolved hyperfine interaction may arise from an SH or from an OH ligand (Fig. 6).

Finally, the High- G state has a g_{av} value similar to the reported value for the S147C mutant of DMSO reductase and the High- G states of nitrate reductase and formate dehydrogenase [16, 33]. We therefore assume that this species has a similar coordination sphere (five sulfur ligands) as described above. The Mo hyperfine pattern observable for the Very-High- G species (see Fig. 1) is not well resolved for this state (Fig. 2C), indicating dynamic or static heterogeneity of this state. The anisotropy of the G -tensor (ΔG) is much larger in Psr, as compared to these other enzymes. Its position in the diagram of Fig. 5 is exactly on the correlation line expected for square pyramidal configuration geometry, implying a highly symmetric arrangement of the two MGDs in the equatorial ligand plane. It accumulates only after extended measurement times with repeated freeze-thaw cycles, but can be converted back to the Very-High- G signal as described above. This may be an indication that this state is not directly involved in the native catalytic reaction and consists of inactive proteins trapped in a Mo^{V} side reaction state.

Conclusion

Three spectroscopically different Mo^{V} states have been observed for the first time in Psr from *W. succinogenes*. They are characterised by their EPR parameters, G -tensor values (g_{av} , ΔG , ε) and hyperfine couplings (A_{Mo} , A_{H}). The influence of the coprotein Sud on the Very-High- G state (Very-High- G /Sud) strongly suggests that this state is an active state in the catalytic reaction of Psr and that the substrate polysulfide is directly

ligated to the Mo ion in this state. On the basis of the EPR parameters obtained and by comparison with other molybdo enzymes, like nitrate reductase, formate dehydrogenase and DMSO reductase, structures for the observed Mo^{V} states are proposed (Fig. 6). Pulsed ESEEM measurements with ^{33}S isotope-labelled polysulfide substrate and quantum theoretical MO calculations to further support our conclusions are in progress.

Acknowledgements This work was supported by the Sonderforschungsbereich "Molecular Bioenergetics" of the Deutsche Forschungsgemeinschaft (DFG, Sfb 472). Axel Weber is thanked for performing the S-band cw-EPR measurements and the EPR division of Bruker, Rheinstetten, for the possibility to perform the Q-band EPR measurements.

References

1. Unden G, Bongaerts J (1997) *Biochim Biophys Acta* 1320:217–234
2. Hedderich R, Klimmek O, Kröger A, Dirmeier R, Keller M, Stetter KO (1999) *FEMS Microbiol Rev* 22:353–381
3. Richardson DJ (2000) *Microbiology* 146:551–571
4. Kröger A, Biel S, Simon J, Gross R, Unden G, Lancaster CRD (2002) *Biochim Biophys Acta* 1553:23–38
5. Schauder R, Kröger A (1993) *Arch Microbiol* 159:491–497
6. Dietrich W, Klimmek O (2002) *Eur J Biochem* 269:1085–1086
7. Krafft T, Bokranz M, Klimmek O, Schröder I, Fahrenholz F, Kojro E, Kröger A (1992) *Eur J Biochem* 206:503–510
8. Kisker C, Schindelin H, Rees DC (1997) *Annu Rev Biochem* 66:233–267
9. McAlpine AS, McEwan AG, Shaw AL, Bailey S (1997) *J Biol Inorg Chem* 2:690–701
10. Li HK, Temple C, Rajagopalan KV, Schindelin H (2000) *J Am Chem Soc* 122:7673–7680
11. Dias JM, Than ME, Humm A, Huber R, Bourenkov GP, Bartunik HD, Bursakov S, Calvete J, Caldeira J, Carneiro C, Moura JGG, Moura I, Ramão MJ (1999) *Structure* 7:65–79
12. Boyington JC, Gladyshev VN, Shagulov SV, Stadtman TC, Sun PD (1997) *Science* 275:1305–1308
13. Baugh PE, Garner CD, Charnock JM, Collison D, Davies ES, McAlpine AS, Bailey S, Lane I, Hanson GR (1997) *J Biol Inorg Chem* 2:634–643
14. George GN, Hilton J, Temple C, Prince RC, Rajagopalan KV (1999) *J Am Chem Soc* 121:1256–1266
15. Butler CS, Charnock JM, Bennet B, Sears HJ, Reilly AJ, Ferguson SJ, Garner CD, Lowe DJ, Thomson AJ, Richardson DJ (1999) *Biochemistry* 38:9000–9012
16. Bray RC (1988) *Rev Biophys* 21:299–329
17. Bennett B, Benson N, McEwan AG, Bray RC (1994) *Eur J Biochem* 225:321–331
18. Bastian NR, Kay CJ, Barber MJ, Rajagopalan KV (1991) *J Biol Chem* 266:45–51
19. George GN, Bray RC (1988) *Biochemistry* 27:3603–3609
20. Wilson GL, Greenwood RJ, Pilbrow JR, Spence JT, Wedd AG (1991) *J Am Chem Soc* 113:6803–6812
21. Balagopalakrishna C, Kimbrough JT, Westmoreland TD (1996) *Inorg Chem* 35:7758–7768
22. Cramer SP, Johnson JL, Rajagopalan KV, Sorrell TN (1979) *Biochem Biophys Res Commun* 91:434–439
23. Greenwood RJ, Wilson GI, Pilbrow JR, Wedd AG (1993) *J Am Chem Soc* 115:5385–5392
24. Hanson GR, Brunette AA, McDonell AC, Murray KS, Wedd AG (1981) *J Am Chem Soc* 103:1953–1959
25. Howes BD, Bennett B, Koppenhöfer A, Lowe DJ, Bray RC (1991) *Biochemistry* 30:3969–3975
26. Howes BD, Bray RC, Richards RL, Turner NA, Bennett B, Lowe DJ (1996) *Biochemistry* 35:1432–1443

27. Malthouse JP, George GN, Lowe DJ, Bray RC (1981) *Biochem J* 199:629–637
28. Howes BD, Pinhal NM, Turner NA, Bray RC, Anger G, Ehrenberg A, Raynor JB, Lowe DJ (1990) *Biochemistry* 29:6120–6127
29. Raitsimring AM, Pacheco A, Enemark JH (1998) *J Am Chem Soc* 120:11263–11278
30. Astashkin AV, Raitsimring AM, Feng C, Johnson JL, Rajagopalan KV, Enemark JH (2002) *J Am Chem Soc* 124:6109–6118
31. Barber MJ, Bray RC, Lowe DJ, Coughlan MP (1976) *Biochem J* 153:297–307
32. Gangeswaran R, Lowe DJ, Eady RR (1993) *Biochem J* 289:335–342
33. Barber MJ, Siegel LM, Schauer NL, May HD, Ferry JG (1983) *J Biol Chem* 258:10839–10845
34. Barber MJ, May HD, Ferry JG (1986) *Biochemistry* 25:8150–8155
35. Khangulov SV, Gladyshev VN, Dismukes GC, Stadtman TC (1998) *Biochemistry* 37:3518–3528
36. Cleland WE, Barnhardt ITM, Yamanouchi K, Collison D, Mabbs FE, Ortega RB, Enemark JH (1987) *Inorg Chem* 26:1017–1025
37. Klimmek O, Kreis V, Klein C, Simon J, Wittershagen A, Kröger A (1998) *Eur J Biochem* 253:263–269
38. Klimmek O, Stein T, Piza R, Simon J, Kröger A (1999) *Eur J Biochem* 263:79–84